

Flux Decline and Fouling Analysis in Reverse Osmosis of Watermelon Juice

Quoc Dat Lai (✉ lqdat@hcmut.edu.vn)

Ho Chi Minh City University of Technology (HCMUT)

Ngoc Thuc Trinh Doan

Ho Chi Minh City University of Technology (HCMUT)

Hoang Dung Nguyen

Ho Chi Minh City University of Technology (HCMUT)

Research Article

Keywords: Reverse osmosis, watermelon juice, concentration, modelling, lycopene, antioxidant activity

Posted Date: March 30th, 2022

DOI: <https://doi.org/10.21203/rs.3.rs-1487272/v1>

License: © ⓘ This work is licensed under a Creative Commons Attribution 4.0 International License.

[Read Full License](#)

1 **FLUX DECLINE AND FOULING ANALYSIS IN REVERSE OSMOSIS OF WATERMELON JUICE**

2 **Lai Quoc Dat^{1,2*}, Doan Ngoc Thuc Trinh^{1,2}, Nguyen Hoang Dung^{1,2}**

3 *Corresponding Authors' email: lqdat@hcmut.edu.vn

- 4 1) Department of Food Technology, Faculty of Chemical Engineering, Ho Chi Minh City University of
5 Technology (HCMUT), 268 Ly Thuong Kiet Street, District 10, Ho Chi Minh City, Vietnam
- 6 2) Vietnam National University Ho Chi Minh City, Linh Trung Ward, Thu Duc District, Ho Chi Minh City,
7 Vietnam

8

9 **Abstract**

10 In this paper, the concentration of watermelon juice by HR98PP membrane was investigated at 30 and 40 bar
11 of operating pressure. The semi-empirical model of permeate flux was determined. The predominant fouling
12 mechanism in the concentration was found to be complete blocking by Hermia's model. Recovery yield and content
13 of total solid, lycopene and antioxidant capacity in concentrate was analyzed. Results indicated that, concentration of
14 watermelon juice by HR98PP at 40 bar exhibited the higher effectiveness than that at 30 bar. At 40 bar and 2.25 of
15 CF, contents of total sugar (TS), lycopene and antioxidant capacity in concentrate were 171.31 g/L, 83.9 mg/L and
16 124.74 mg TEAC/L, respectively. Recovery yields of TS, lycopene and antioxidant capacity in concentrate were
17 98.67. 90.03 and 82.39 %, respectively. Maximum CF value of concentration at 40 bar of operating pressure was 2.64.
18 The mathematical model was built for estimation of the change in the contents of lycopene and TS versus time.
19 Maximum theoretical content of lycopene and TS at 40 bar were estimated as 185 mg/L and 341 g/L, respectively.
20 The cleaning procedure with NaOH solution at pH10 could fully recovery permeate flux after the concentration.
21 Results imply that, concentration of watermelon juice by HR98PP was feasible.

22

23 **Keywords:** Reverse osmosis; watermelon juice; concentration; modelling; lycopene; antioxidant activity.

24

25

26 **1. Introduction**

27 Watermelon (*Citrullus lanatus*) is a fruit with high content of lycopene: 8.20 – 59.17 mg/100 g watermelon
28 flesh (Oberoi and Sogi 2017). Due to richness of lycopene, watermelon juice exhibits the high antioxidant capacity
29 (Neglo et al. 2021). Di Mascio et al. (1991) and Ribaya-Mercado et al. (1995) reported that lycopene exhibits the
30 quenching capacity of singlet oxygen in vitro with quenching constant being 2 and 10 times higher than that of β –
31 carotene and α – tocopherol. Lycopene-rich foods are considered to relate to a lower risk of some degeneration
32 diseases (Liang et al. 2019). Lycopene plays roles as a chemopreventive agent of digestive-tract cancers, lung cancer
33 and prostate cancer (Anlar and Bacanli 2020; Bano et al. 2020; Mirahmadi et al. 2020; Qi et al. 2021). However,
34 thermal processes cause the isomerization, consequently, reduction of biological activity of lycopene (Gupta et al.
35 2010; Murakami et al. 2018; Saini et al. 2019). Watermelon juice is also a source of citrulline with content being 1.1
36 – 4.7 g/kg in flesh (Tarazona-Díaz et al. 2011). Citrulline is precursor for arginine for human (Bahadoran et al. 2020).
37 In addition, watermelon juice contains many nutritious constituents, such as: vitamins (A, B1, B2, B6, C, E) and
38 minerals (Maoto et al. 2019). In general, watermelon juice is an extremely valuable source of nutrition for human
39 health.

40 Recently, watermelon juice has been consumed in form of fresh juice, concentrate and instant powder. In
41 concentrate and instant powder production juice, the concentration is one of the most important steps because it
42 determines quality and energy consumption. Recently, concentration of juice has been conducted by vacuum
43 evaporation. However, thermally sensitive constituents are destroyed by influence of high temperature. With lycopene,
44 thermal processes cause the isomerization and oxidation, consequently, reduction of biological activity (Colle et al.
45 2013; Murakami et al. 2018; Saini et al. 2019). In addition, sensory properties of juice, especially flavor, is significant
46 change under thermal processing (Pendyala et al. 2020). Consequently, it leads to decrease in quality of final products.

47 Reverse osmosis (RO) is membrane separation process with pressure driving force. The mechanisms of
48 separation are based on sieving and diffusion effects (Wenten and Khoiruddin 2016). This process can be conducted
49 at ambient temperature, thus remains the thermally sensitive compounds (W. Barker 2011). Besides, RO process
50 consumes lower energy than the evaporation (Cassano et al. 2021). In addition, the RO system is also low capital cost,
51 easy to install, operate and maintain (Anis et al. 2019). Because of these advantages, RO process has been used to
52 concentrated a variety of juices, e.g. apple (Ahmad et al. 2020), orange (Destani et al. 2020), pomegranate (Bagci et
53 al. 2020), etc. Dos Santos Gomes et al., 2011 evaluated the concentration of watermelon juice by polyamide composite

54 RO membrane. The results showed that the process concentrated juice from 6.5 to 24 °Brix and increased lycopene
55 content 3.1 times. However, this study did not clearly show the impact of operating condition and kinetic in process
56 of concentrating watermelon by RO membrane. Meanwhile, these information help to easily optimize the operation
57 process.

58 The objective of this research was to investigate the application of RO for concentration of watermelon juice.
59 Influence of operating pressure on performance of process was studied. The recovery yield of total sugar (TS),
60 lycopene, and antioxidant capacity in concentration by RO membrane was also determined. The determination of
61 predominant fouling mechanisms and the mathematical models were also investigated to describe the watermelon
62 juice concentration by RO membrane. We aim to assess the feasibility of RO process for concentration of watermelon
63 juice.

64 **2. Materials and methods**

65 **2.1. Materials**

66 **Watermelon juice:** Watermelon (*Citrullus lanatus*) fruits were purchased from a local market in Ho Chi Minh
67 City (Vietnam). Their weight was 3 – 4 kg per fruit, with total red flesh. The fruits were clean by water. Then, it was
68 peeled, followed by recovering flesh. The flesh was crushed by a steel sieve with 1 mm of mesh to obtain the juice.
69 The juice was stored at 4 °C and using in 24 hours.

70 **2.3. Membrane**

71 Reverse osmosis membrane was HR98PP, a composite membrane made from polypropylene, manufactured by
72 Alfa Laval (Denmark). NaCl rejection by this membrane is higher than 96% at 2,000 ppm of NaCl, 15.5 bar of
73 operating pressure and 25 °C of operation temperature (information supplied by manufacturer). Prior to use, membrane
74 was cleaned as following procedure: Flush with clean water with approximately 5 times of the system hold up volume;
75 then, flush by full recirculation of NaOH solution (pH10) in 30 min without applied pressure and 15 L/min of feed
76 flowrate; finally, flush with clean water at 5 bar of applied pressure until pH of permeate and retentate reached 6.0 –
77 7.0.

78 **2.4. Membrane apparatus**

79 The Labstak M20, a plate and frame system manufactured by Alfa Laval (Denmark) was used to carry out the
80 concentration of watermelon juice (**Fig. 1**). The unit consisted of 4 couples of membrane sheets with 0.144 m² of
81 active area (0.018 m²/sheet). The pressure was supplied by Hydra – Cell pump, a piston pump manufactured by

82 Wanner Engineering Inc. (USA). The operating temperature was at ambient. The system was operated as concentration
 83 mode with full recirculation of retentate (**Fig. 1**). Feed flow rate was 15 L/min. In this research, the operation pressure
 84 was investigated at 30 and 40 bar to evaluate the effects of operating pressure on the RO filtration. All experiments of
 85 concentration were in duplicate with difference in permeate flux being lower than 5%.

86 Concentration factor (CF) was expressed as the ratio of initial volume of feed (V_F , L) to the volume of the
 87 retentate (V_R , L):

$$CF = \frac{V_F}{V_R} \quad (1)$$

88 The recovery yield of component i in retentate side (Y) was expressed as the following formula:

$$Y_i = \frac{C_{R,i}V_R}{C_{F,i}V_F} \quad (2)$$

89 Where, $C_{R,i}$ and $C_{F,i}$ were contents (g/L) of component i in retentate and feed, respectively.

90 After each run of RO, crossflow membrane system was cleaned as the following procedure:

- 91 - Flush with clean water with approximately 5 times of the system hold up volume.
- 92 - Recirculate clean water in 30 min at 5 bar of applied pressure and 15 L/min of feed flowrate.
- 93 - Recirculate NaOH solution (pH10) in 30 min without applied pressure and 15 L/min of feed flowrate.
- 94 - Flush with clean water at 5 bar of applied pressure until pH of permeate and retentate was 6.0 – 7.0.

95 2.5. Fouling mechanisms analysis

96 In this work, the fouling mechanism was determined using the models described by Hermia (Equation (3) and
 97 **Table 1**). The equation was determined by nonlinear regression, the coefficient of determination (R^2) and the root
 98 mean square deviation (RMSE) was used to find out the mechanism for each assay evaluated.

$$\frac{d^2t}{dV^2} = k_n \left(\frac{dt}{dV} \right)^n \quad (3)$$

99 Where, n : blocking index, t : filtration time (h), V : accumulated permeate volume (L), k_n : resistance coefficient.

100 Besides that, fouling and cleaning effectiveness in NF were evaluated by fouling and recovery indices and
 101 expressed as the following equations:

102 *Fouling index:*

$$FI = 100 \frac{PWP_{final}}{PWP_{initial}} \quad (4)$$

103 Where, $PWP_{initial}$ ($L.m^{-2}h^{-1}$) and PWP_{final} ($L.m^{-2}h^{-1}$) were the initial pure water permeability of membrane and
104 the pure water permeability when NF was completed.

105 *Recovery index:*

$$RI = 100 \frac{PWP_{cleaning}}{PWP_{initial}} \quad (5)$$

106 Where, $PWP_{initial}$ ($L.m^{-2}h^{-1}$) and $PWP_{cleaning}$ ($L.m^{-2}h^{-1}$) were the initial pure water permeability of membrane
107 and the pure water permeability when the cleaning was completed.

108 **2.7. Mathematical model**

109 In order to model the permeate flux in concentration of watermelon juice by RO process, the following equation
110 was applied:

$$J_v = k \cdot \ln\left(\frac{\alpha}{CF}\right) \quad (6)$$

111 Where, J_v : permeate flux ($L.m^{-2}.h^{-1}$), k : representative of mass transfer in boundary layer on membrane surface
112 ($L.m^{-2}.h^{-1}$) and α : considered as maximum of CF value.

113 This semi – empirical model derived from osmotic pressure model (Nabetani et al. 1995). In osmotic pressure
114 model, permeate flux is limited by difference in osmotic pressure between two sides of membrane. When CF reaches
115 α value, the difference in osmotic pressure between two sides of membrane equals to transmembrane pressure,
116 consequently, permeate flux is zero. This model was successfully applied for modeling permeate flux in concentration
117 chicken extract (Nabetani et al. 2012) and nanofiltration for concentration of fish sauce (Lai and Nguyen 2021), coffee
118 extract (Pan et al. 2013).

119 The variation of retentate volume (V_R , L) during the concentration by membrane filtration:

$$\frac{dV_R}{dt} = -AJ_v \quad (7)$$

120 Where, A: the membrane area (m^2), J_v : permeate flux ($L/m^2.h$)

121 According to the mass balance, the following equation describes the relationship between individual solute
122 variation in retentate flows:

$$\frac{d(V_R C_{R,i})}{dt} = -AJ_v C_{R,i} (1 - R_i) \quad (8)$$

123 Where: R_i : solute retention (-); R_i , A, V_R and $C_{R_o,i}$ were determined from experimental data. The set of equations
124 (equation (7) and equation (8)) were solve by the fourth order Runge – Kutta method in Matlab software (version

125 R2018a). This mathematical model has been successfully applied in modeling in concentration waste fresh tea leaf
126 extract by RO (Lai et al. 2021), as well as purification and concentration rice protein by ultrafiltration (Doan and Lai
127 2021).

128 **2.6. Analytical methods**

129 Total sugar (TS) content of watermelon juice was determined by using sulfuric acid to form furan compounds,
130 then adding phenol as indicator. The absorbance at 490 nm of wavelength was measured (Nielsen 2010).

131 Lycopene: Total lycopene were analyzed by spectrometric method (Fish et al. 2002). 10 mL of n-hexane was
132 delivered into a tube. Then, adding 5 mL of ethanol 95% (v/v) and 5 mL of BHT 0.05% (w/v) in acetone. The mixture
133 was vortexed. A given weight (approximately 0.5 gram) of watermelon juice was added into the mixture and shaking
134 at 180 rpm in 15 min. Then, 3 mL of distilled water was added and shaking at 180 rpm in 5 min. After shaking, the
135 tube was remained in 5 min for phase separation. Three mL of upper layer (n-hexane) was taken to determine the
136 absorbance at 403 nm of wavelength. All steps were conducted at 20 °C. Content of lycopene was calculated by the
137 following equation:

$$Lycopene (mg/kg) = \frac{A_{503} \times 31.2}{m_{juice} (g)} \quad (9)$$

138 Antioxidant capacity of watermelon juice was determined as the scavenging capacity of 1,1-diphenyl-2-
139 picrylhydrazyl (DPPH) (Oms-Oliu et al. 2009). Watermelon juice was centrifuged at 6000g for 15 min at 4 °C. Then,
140 0.01 mL of the supernatant was added to 3.9 mL of 0.025 g/L of DPPH in methanol. Then, adding 0.090 mL of distilled
141 water. The mixture was vortexed and kept in 30 mins in darkness. Then, the absorbance was determined at 515 nm of
142 wavelength. Blank was methanol. AC was estimated as mg/L of Trolox equivalent antioxidant capacity (TEAC).

143 **3. Results and discussion**

144 **3.1. Permeate flux**

145 Permeate flux in concentration of watermelon juice by HR98PP was showed in **Fig. 2**. Permeate flux declined
146 with increase in CF. Due to higher driving force, at same CF value, permeate flux at 40 bar was higher than that at 30
147 bar of operating pressure. At initial point, permeate flux at 40 bar was 19.74 L.m⁻².h⁻²; whereas, that at 30 bar was
148 13.54 L.m⁻².h⁻². The curves of permeate flux at 30 and 40 bar of operating pressure was nearly offset. It means that
149 the difference in permeate flux decline between at 30 and 40 bar of operating pressure was insignificant during the
150 concentration. It implies that, based on resistance series model, influence of operating pressure on fouling in

151 concentration by HR98PP was also insignificant (W. Barker 2011). It also implies that, increase in total solid in
152 retentate insignificantly influenced on concentration polarization due to the high turbulence of fluid on membrane
153 surface. Thus, the decline of permeate flux with increase in CF can be explained by increase in osmotic pressure,
154 which caused by increase in total solid in retentate.

155 Based on equation (6), the linear regression was applied for modeling of permeate flux. Result in **Fig. 2** and **Fig.**
156 **3** and the approximate 1.0 of R^2 indicates that model exhibited the good agreement with experimental data. The
157 estimation of value in concentration of watermelon juice by HR98PP was stated in **Table 2**. The mass transfer (k)
158 value at 30 bar was lower than that at 40 bar. Wijmans et al. (1984) proved that increase in operating pressure leads
159 to increase in mass transfer in boundary layer on membrane surface. And result in **Table 2** also indicates that higher
160 operating pressure lead to higher maximum value of CF due to higher transmembrane pressure.

161 The statistical analysis results are summarized in **Table 3**. The resistance coefficient (k_n), coefficient of
162 determination (R^2) and the root mean square deviation (RMSE) were used to compare the numerical predictions and
163 the experimental data, and to choose the best fit mechanism for fouling and permeate decline over time evaluation.
164 The results showed that blocking models were better correlated with experimental results than cake filtration models.
165 This was completely consistent with the explanation for flux variation as a function of concentration factor. At both
166 survey pressure conditions, the complete blocking model had the highest R^2 value, and best fit to the experimental
167 data. On the other hand, the standard blocking mechanism had the highest resistance coefficient indicating that it was
168 the most important fouling mechanism. For standard blocking the R^2 was about 0.986 and 0.946, respectively, at 30
169 and 40 bar that also showed the good agreement between the model and the experimental data. This is explained that
170 the watermelon juice is a complex solution containing solutes of varying sizes, the multiple pore blockings
171 mechanisms can occur simultaneously. This phenomenon reported in concentration of strawberry juice by Arend,
172 Rezzadori, et al. (2019). However, due to the molecular weight of components in the watermelon juice, as well as the
173 high operating pressure (30 – 40 bar), the foulants were less likely to enter the pore and reduce diameter. Therefore,
174 the standard pore blocking did not occur significantly. This was also observed in several other studies (Lamdande et
175 al. 2020; Lin 2017).

176 The resistance coefficient of the cake filtration mechanism was extremely low, indicating that there was no
177 boundary layer formation in the concentration of watermelon juice. This reaffirmed that, as total solid concentration
178 increased, concentration polarization had no significant effect on permeate flux. This suggested that the complete

179 blocking mechanism is dominant during concentration of watermelon juice. Both complete pore blocking and cake
180 filtration mechanism occur when the sizes of most solute molecules in watermelon juice were greater than the
181 membrane pore size. As results, particles are unable to enter into the pore and permeate through the membrane (Khan
182 et al. 2020). However, cake layer occurs in the presence of factors such as high concentration and binding of molecules,
183 binding to the membrane and they can deposit on the membrane surface. It has a great influence on the permeate flux.
184 While, in the case of the complete blocking mechanisms, a molecule never settles on another molecule that has
185 previously deposited on the membrane surface (Vela et al. 2008). It is easily eliminated by strong impacts such as
186 high pressure or turbulent flow, and it has little effect on permeate flux. These prove that HR98PP membranes were
187 suitable for watermelon juice concentration. Furthermore, the resistance coefficient was greater at 40 bar of operating
188 pressure than at 30 bar. This suggested that the increased pressure was responsible for the increase in turbulent flow,
189 thereby reducing fouling phenomena. The complete blocking mechanism has also observed in many concentration
190 processes by RO, such as waste fresh tea leaf extract (Lai et al. 2021), skim milk (Arend, Castoldi, et al. 2019).

191 **3.2. Recovery yields and contents of components in retentate**

192 Content in retentate and recovery yield of TS in concentration of watermelon juice by HR98PP is showed in **Fig.**
193 **4.** Relationship between TS content and CF was linear. It means that, rejection of TS was insignificant change in
194 concentration of the juice. However, slope of TS content versus CF at 30 bar was slightly lower than at 40 bar. It
195 implies that rejection of TS at 30 bar was lower than that at 40 bar. Tsuru et al. (1991) proved that, increase in operating
196 pressure leads to increase in rejection in RO process. Comparing to at 40 bar, at 30 bar, the lower rejection of TS led
197 to the lower recovery yield. At 40 bar, recovery yield was 98.6% when reaching 2.25 of CF; whereas, at 30 bar, the
198 one was 90.7% when reaching 1.78 of CF. Ratio of C_R/C_F to CF at 40 bar was approximately 1.0. It means that,
199 rejection of TS at 40 bar was approximately 100%. Whereas, that ratio at 30 bar was higher than 0.92, implies that
200 rejection of TS at 30 bar was higher than 92%. The high rejection of TS also led to low concentration of TS in permeate
201 (**Fig. 5**). Result in **Fig. 5** indicates that, content of TS in permeate was very lower than one in retentate. At 40 bar of
202 operating pressure and 2.25 of CF, TS content in permeate was 2.41 g/L. The one at 30 bar of operating pressure and
203 1.79 of CF was 1.93 g/L. At same CF value, TS content in permeate at 30 bar of operating pressure was higher than
204 that at 40 bar because that, rejection of TS at 30 bar was lower than that at 40 bar.

205 Estimation based on equation (6) indicates that, maximum of CF in retentate could reach 2.6 folds higher than
206 that in feed. Dos Santos Gomes et al. (2011) reported that, when concentrating watermelon juice by RO membrane at

207 60 bar, CF and TS content can reach 4.4 and 30 °Brix, 3.2 folds in relation to feed. The CF and TS content in that
208 work was higher than ones in our work. Nevertheless, the process carried out by Dos Santos Gomes et al. (2011) was
209 conducted at higher operating pressure and recovery of TS was lower, in comparing with present work.

210 Content and recovery yield of lycopene in concentration of watermelon juice by HR98PP is showed in **Fig. 6**.
211 Rejection of lycopene in RO process insignificantly changed due to linear relationship between lycopene content and
212 CF. Result also indicates that, lycopene in permeate was not detected. At 2.25 of CF and 40 bar of operating pressure,
213 recovery yield of lycopene was 90%. Whereas, at 1.79 of CF and 30 of operating pressure, the one was 86.8%. It
214 means that, there was the loss of lycopene by oxidation resulted in a reduction in recovery yield along with increase
215 in CF. Comparing at 40 bar, the recovery yield of lycopene at 30 bar was lower due to operating time at 30 bar was
216 longer. The loss of lycopene by oxidation and isomerization reactions was also observed in report by Dos Santos
217 Gomes et al. (2011). However, the loss of lycopene in membrane process was not much as comparing to concentration
218 by evaporation. The concentration of watermelon juice from 8 °Brix to 30 °Brix at 50 °C and 100 mg Hg of pressure
219 in rotary vacuum evaporator, 33.7% of lycopene was degraded (Jaju et al. 2017).

220 The processing properties of watermelon juice in concentration at 30 and 40 bar based on proposed mathematical
221 model are presented in **Fig. 7**. The theoretical results are given from mathematical models that were well consistent
222 with the experimental data. The content of lycopene and TS at 40 bar was higher than that at 30 bar due to the faster
223 concentration process caused by the higher permeate flux. It implies that, at 40 bar, the concentration of watermelon
224 juice was more effective compared to at 30 bar. In mathematical model, rejection was assumed to be constant and
225 estimated as mean of experimental rejection, and permeate flux varied linearly with CF, but experimental rejection
226 and permeate flux slightly changed. As a result, there is a discrepancy between calculating data and measured data.
227 However, they fluctuated slightly and asymptotically around the predicted value. The reasons for this were the fouling
228 phenomena that cough occur after a time of operation and increase in the viscosity of the retentate. Thus, the predictive
229 model can be used to predict the time operation for a target solutes concentration at the end of the concentration. From
230 the mathematical model, the maximum theoretical value of lycopene content at 30 and 40 bar were 172 and 185 mg/L,
231 respectively, increased by 4.5 and 3.5 folds, with operating time of 36.8 and 27.1 hours. Along with that, the maximum
232 of TS content was 245 and 341 g/L, respectively. It implies that, the concentration of watermelon juice was more
233 effective at 40 bar, due to shorter time and higher of molecules content. Compared with other studies on applying RO
234 for concentration, the maximum theoretical value of TS content obtained at 40 bar in watermelon juice concentration

235 by HR98PP membrane is significantly higher than soluble solids content obtained in concentration by RO membrane
236 of orange juice (30 °Brix at 60 bar, (Jesus et al. 2007), apple juice (28.1 °Brix at 60 bar, (Aguiar et al. 2012)),
237 chokeberry juice (24.9 °Brix at 55 bar, (Pozderović et al. 2016)), pomegranate juice (18 °Brix at 30 bar, (Bagci et al.
238 2019)). The maximum theoretical value of lycopene and TS content in watermelon juice obtained by concentration
239 with HR98PP membrane suggests that, the concentrate exhibited a good recovery particles which could be used in
240 another process without concentrated process more. However, more research is necessary to identify the optimal multi-
241 stage RO system for a watermelon juice product with high concentration of bioactive compounds and soluble solids.

242 Summary of concentration of watermelon juice by HR98PP was stated in **Table 4**. Result in **Table 4** indicated
243 that the antioxidant capacity of watermelon juice was lost 29.89 and 17.61% when concentration by RO at 30 bar,
244 1.79 of CF and 40 bar, 2.25 of CF, respectively. Result also indicated that, the fouling in RO process with HR98PP at
245 30 bar of operating pressure was more severe than that at 40 bar. FI values of RO process at 30 bar and 40 bar were
246 67.11 and 76.64% . However, the cleaning as proposed procedure was eliminated fouling. RI values of RO process
247 with HR98PP at 30 and 40 bar of operating pressure were higher than 95%. It means that, permeate flux was fully
248 recovered.

249 **4. Conclusions**

250 Results indicated that the concentration of watermelon juice by HR98PP at 40 bar of operating pressure was
251 more effective than that at 30 bar. The semi-empirical model has shown good performance when used to simulate
252 permeate flux. The complete blocking mechanism was observed to be the reason causing fouling phenomena and the
253 decline in permeate flux in concentration of watermelon juice by HR98PP. Theoretical maximum value of CF was
254 2.64. Recovery yields of TS, lycopene and antioxidant at 40 bar of operating pressure and 2.25 of CF were 98.67,
255 90.03 and 82.39, respectively. Result showed that, at 40 bar, the maximum contents of lycopene and TS increased up
256 to 4.5 folds. TS and lycopene contents at that conditions of RO process were 171.31 g/L and 83.90 mg/L, respectively.
257 From mathematical model, the theoretical permeate flux, content of compounds in retentate over time were observed,
258 and they were in good agreement with the experimental data. The fouling in RO process were severe; however,
259 cleaning with NaOH solution at pH10 was fully eliminated fouling. It is feasible to utilize HR98PP membrane for
260 concentration of watermelon juice.

261 **ACKNOWLEDGEMENT**

262 We acknowledge the support of time and facilities from Ho Chi Minh City University of Technology (HCMUT),
263 VNU–HCM for this study.

264 **CONFLICT OF INTEREST**

265 None

266 **ETHICAL APPROVAL**

267 Ethics approval was not required for this research.

268 **DATA AVAILABILITY STATEMENT**

269 Data available on request from the authors.

270 **AUTHOR’S CONTRIBUTION STATEMENT**

271 Q.D.L and H.D.N designed and directed the project. Q.D.L and N.T.T.D. wrote the main manuscript text.
272 N.T.T.D. processed the experimental data, performed the analysis. All authors reviewed the manuscript.

273 **REFERENCES**

274 Aguiar, I. B., Miranda, N. G. M., Gomes, F. S., Santos, M. C. S., de GC Freitas, D., Tonon, R. V., & Cabral, L. M. C.
275 (2012). Physicochemical and sensory properties of apple juice concentrated by reverse osmosis and osmotic
276 evaporation. *Innovative Food Science & Emerging Technologies*, 16, 137–142.

277 Ahmad, S., Marson, G. V., Zeb, W., Rehman, W. U., Younas, M., Farrukh, S., & Rezakazemi, M. (2020). Mass
278 transfer modelling of hollow fiber membrane contactor for apple juice concentration using osmotic membrane
279 distillation. *Separation and Purification Technology*, 117209.

280 Anis, S. F., Hashaikeh, R., & Hilal, N. (2019). Reverse osmosis pretreatment technologies and future trends: A
281 comprehensive review. *Desalination*, 452, 159–195.

282 Anlar, H. G., & Bacanli, M. (2020). Lycopene as an antioxidant in human health and diseases. In *Pathology* (pp. 247–
283 254). Elsevier.

284 Arend, G. D., Castoldi, S. M., Rezzadori, K., Soares, L. S., & Brião, V. B. (2019). Concentration of skim milk by
285 reverse osmosis: characterization and flow decline modelling. *Brazilian Journal of Food Technology*, 22.

286 Arend, G. D., Rezzadori, K., Soares, L. S., & Petrus, J. C. C. (2019). Performance of nanofiltration process during
287 concentration of strawberry juice. *Journal of food science and technology*, 56(4), 2312–2319.

288 Bagci, P. O., Akbas, M., Gulec, H. A., & Bagci, U. (2019). Coupling reverse osmosis and osmotic distillation for

289 clarified pomegranate juice concentration: Use of plasma modified reverse osmosis membranes for improved
290 performance. *Innovative Food Science & Emerging Technologies*, 52, 213–220.

291 Bagci, P. O., Kahvecioglu, H., Gulec, H. A., & Bagci, U. (2020). Pomegranate juice concentration through the
292 consecutive application of a plasma modified reverse osmosis membrane and a membrane contactor. *Food and*
293 *Bioproducts Processing*, 124, 233–243.

294 Bahadoran, Z., Mirmiran, P., Kashfi, K., & Ghasemi, A. (2020). Endogenous flux of nitric oxide: Citrulline is preferred
295 to Arginine. *Acta Physiologica*, e13572.

296 Bano, S., Ahmed, F., Khan, F., Chaudhary, S. C., & Samim, M. (2020). Targeted delivery of thermoresponsive
297 polymeric nanoparticle-encapsulated lycopene: in vitro anticancer activity and chemopreventive effect on
298 murine skin inflammation and tumorigenesis. *RSC Advances*, 10(28), 16637–16649.

299 Cassano, A., Castro-Muñoz, R., Conidi, C., & Drioli, E. (2021). Recent Developments in Membrane Technologies
300 for Concentration of Liquid Foods and Food Ingredients. In K. Knoerzer & K. B. T.-I. F. P. T.
301 Muthukumarappan (Eds.), *Innovative Food Processing Technologies: A comprehensive Review* (pp. 100–121).
302 Oxford: Elsevier. <https://doi.org/https://doi.org/10.1016/B978-0-08-100596-5.23036-9>

303 Colle, I. J. P., Lemmens, L., Van Buggenhout, S., Van Loey, A. M., & Hendrickx, M. E. (2013). Modeling lycopene
304 degradation and isomerization in the presence of lipids. *Food and Bioprocess Technology*, 6(4), 909–918.

305 Destani, F., Naccarato, A., Tagarelli, A., & Cassano, A. (2020). Recovery of Aromatics from Orange Juice Evaporator
306 Condensate Streams by Reverse Osmosis. *Membranes*, 10(5), 92.

307 Di Mascio, P., Murphy, M. E., & Sies, H. (1991). Antioxidant defense systems: the role of carotenoids, tocopherols,
308 and thiols. *The American Journal of Clinical Nutrition*, 53(1), 194S-200S.
309 <https://doi.org/10.1093/ajcn/53.1.194S>

310 Doan, N. T. T., & Lai, Q. D. (2021). Ultrafiltration for recovery of rice protein : Fouling analysis and technical
311 assessment. *Innovative Food Science and Emerging Technologies*, 70, 102692.
312 <https://doi.org/10.1016/j.ifset.2021.102692>

313 Dos Santos Gomes, F., Albuquerque da Costa, P., Domingues de Campos, M. B., Couri, S., & Cabral, L. M. C. (2011).
314 Concentration of watermelon juice by reverse osmosis process. *Desalination and Water Treatment*, 27(1–3),
315 120–122.

316 Fish, W. W., Perkins-Veazie, P., & Collins, J. K. (2002). A quantitative assay for lycopene that utilizes reduced

317 volumes of organic solvents. *Journal of food composition and analysis*, 15(3), 309–317.

318 Gupta, R., Balasubramaniam, V. M., Schwartz, S. J., & Francis, D. M. (2010). Storage stability of lycopene in tomato
319 juice subjected to combined pressure– heat treatments. *Journal of agricultural and food chemistry*, 58(14),
320 8305–8313.

321 Jaju, N. S., Patel, S. S., Birwal, P., Deshmukh, G., Sukhdev, B. S., & Nema, P. K. (2017). Effect of Vacuum
322 Evaporation Concentration on Lycopene Content and Rheological Properties of Watermelon Juice. *Int. J. Pure*
323 *App. Biosci*, 5(3), 1018–1024.

324 Jesus, D. F., Leite, M. F., Silva, L. F. M., Modesta, R. D., Matta, V. M., & Cabral, L. M. C. (2007). Orange (Citrus
325 sinensis) juice concentration by reverse osmosis. *Journal of Food Engineering*, 81(2), 287–291.

326 Khan, I. A., Lee, Y.-S., & Kim, J.-O. (2020). A comparison of variations in blocking mechanisms of membrane-
327 fouling models for estimating flux during water treatment. *Chemosphere*, 259, 127328.

328 Lai, Q. D., Doan, N. T. T., & Nguyen, H. D. (2021). Technical assessment of reverse osmosis for concentration of
329 fresh tea leaf extract. *Journal of Food Process Engineering*, 44(7), e13725.

330 Lai, Q. D., & Nguyen, H. D. (2021). Enhancement of fish sauce quality by application of nanofiltration. *LWT*,
331 151(January), 112181. <https://doi.org/10.1016/j.lwt.2021.112181>

332 Lamdande, A. G., Mittal, R., & K.S.M.S., R. (2020). Flux evaluation based on fouling mechanism in acoustic field-
333 assisted ultrafiltration for cold sterilization of tender coconut water. *Innovative Food Science and Emerging*
334 *Technologies*, 61, 102312. <https://doi.org/10.1016/j.ifset.2020.102312>

335 Liang, X., Ma, C., Yan, X., Liu, X., & Liu, F. (2019). Advances in research on bioactivity, metabolism, stability and
336 delivery systems of lycopene. *Trends in Food Science & Technology*, 93, 185–196.

337 Lin, Y. L. (2017). Effects of organic, biological and colloidal fouling on the removal of pharmaceuticals and personal
338 care products by nanofiltration and reverse osmosis membranes. *Journal of Membrane Science*, 542, 342–351.
339 <https://doi.org/10.1016/j.memsci.2017.08.023>

340 Maoto, M. M., Beswa, D., & Jideani, A. I. O. (2019). Watermelon as a potential fruit snack. *International Journal of*
341 *food properties*, 22(1), 355–370.

342 Mirahmadi, M., Azimi-Hashemi, S., Saburi, E., Kamali, H., Pishbin, M., & Hadizadeh, F. (2020). Potential inhibitory
343 effect of lycopene on prostate cancer. *Biomedicine & Pharmacotherapy*, 129, 110459.

344 Murakami, K., Honda, M., Takemura, R., Fukaya, T., Kanda, H., & Goto, M. (2018). Effect of thermal treatment and

345 light irradiation on the stability of lycopene with high Z-isomers content. *Food chemistry*, 250, 253–258.

346 Nabetani, H., Abbott, T. P., & Kleiman, R. (1995). Optimal Separation of Jojoba Protein Using Membrane Processes.

347 *Industrial and Engineering Chemistry Research*, 34(5), 1779–1788. <https://doi.org/10.1021/ie00044a029>

348 Nabetani, H., Hagiwara, S., Yanai, N., Shiotani, S., Baljinnyam, J., & Nakajima, M. (2012). Purification and

349 concentration of antioxidative dipeptides obtained from chicken extract and their application as functional food.

350 *Journal of Food and Drug Analysis*, 20(SUPPL.1), 179–183. <https://doi.org/10.38212/2224-6614.2145>

351 Neglo, D., Tettey, C. O., Essuman, E. K., Kortei, N. K., Boakye, A. A., Hunkpe, G., et al. (2021). Comparative

352 antioxidant and antimicrobial activities of the peels, rind, pulp and seeds of watermelon (*Citrullus lanatus*) fruit.

353 *Scientific African*, 11, e00582.

354 Nielsen, S. S. (2010). Phenol-sulfuric acid method for total carbohydrates. In *Food analysis laboratory manual* (pp.

355 47–53). Springer.

356 Oberoi, D. P. S., & Sogi, D. S. (2017). Utilization of watermelon pulp for lycopene extraction by response surface

357 methodology. *Food chemistry*, 232, 316–321.

358 Oms-Oliu, G., Odriozola-Serrano, I., Soliva-Fortuny, R., & Martín-Belloso, O. (2009). Effects of high-intensity pulsed

359 electric field processing conditions on lycopene, vitamin C and antioxidant capacity of watermelon juice. *Food*

360 *chemistry*, 115(4), 1312–1319.

361 Pan, B., Yan, P., Zhu, L., & Li, X. (2013). Concentration of coffee extract using nanofiltration membranes.

362 *Desalination*, 317, 127–131.

363 Pendyala, B., Patras, A., Ravi, R., Gopisetty, V. V. S., & Sasges, M. (2020). Evaluation of UV-C irradiation treatments

364 on microbial safety, ascorbic acid, and volatile aromatics content of watermelon beverage. *Food and Bioprocess*

365 *Technology*, 13(1), 101–111.

366 Pozderović, A., Popović, K., Pichler, A., & Jakobek, L. (2016). Influence of processing parameters on permeate flow

367 and retention of aroma and phenolic compounds in chokeberry juice concentrated by reverse osmosis. *CyTA-*

368 *Journal of Food*, 14(3), 382–390.

369 Qi, W. J., Sheng, W. S., Peng, C., Xiaodong, M., & Yao, T. Z. (2021). Investigating into anti-cancer potential of

370 lycopene: Molecular targets. *Biomedicine & Pharmacotherapy*, 138, 111546.

371 Ribaya-Mercado, J. D., Garmyn, M., Gilchrest, B. A., & Russell, R. M. (1995). Skin lycopene is destroyed

372 preferentially over β -carotene during ultraviolet irradiation in humans. *The Journal of nutrition*, 125(7), 1854–

373 1859.

374 Saini, R. K., A. Bekhit, A. E.-D., Roohinejad, S., Rengasamy, K. R. R., & Keum, Y.-S. (2019). Chemical stability of
375 lycopene in processed products: A review of the effects of processing methods and modern preservation
376 strategies. *Journal of agricultural and food chemistry*, 68(3), 712–726.

377 Tarazona-Díaz, M. P., Viegas, J., Moldao-Martins, M., & Aguayo, E. (2011). Bioactive compounds from flesh and
378 by-product of fresh-cut watermelon cultivars. *Journal of the Science of Food and Agriculture*, 91(5), 805–812.

379 Tsuru, T., Nakao, S., & Kimura, S. (1991). Calculation of ion rejection by extended Nernst-Planck equation with
380 charged reverse osmosis membranes for single and mixed electrolyte solutions. *JOURNAL OF CHEMICAL*
381 *ENGINEERING OF JAPAN*, 24(4), 511–517. <https://doi.org/10.1252/jcej.24.511>

382 Vela, M. C. V., Blanco, S. Á., García, J. L., & Rodríguez, E. B. (2008). Analysis of membrane pore blocking models
383 applied to the ultrafiltration of PEG. *Separation and Purification Technology*, 62(3), 489–498.
384 <https://doi.org/10.1016/j.seppur.2008.02.028>

385 W. Barker, R. (2011). *Membrane technology and applications*. (R. W. Barker, Ed.) *Membrane Technologies and*
386 *Applications*. England: John Wiley & Sons, Ltd. <https://doi.org/10.1201/b11416>

387 Wenten, I. G., & Khoiruddin. (2016). Reverse osmosis applications: Prospect and challenges. *Desalination*, 391, 112–
388 125. <https://doi.org/10.1016/j.desal.2015.12.011>

389 Wijmans, J. G., Nakao, S., & Smolders, C. A. (1984). Flux limitation in ultrafiltration: Osmotic pressure model and
390 gel layer model. *Journal of Membrane Science*, 20(2), 115–124. [https://doi.org/10.1016/S0376-7388\(00\)81327-](https://doi.org/10.1016/S0376-7388(00)81327-7)
391 7

392

393

394 **FIGURE LEGENDS**

395 **Fig. 1.** Schema of flat and frame pilot LabstakM20 system. 1: feed tank, 2: pump, 3: pressure gauge, 4:
396 membranes, 5: permeate tank, 6: flowmeter

397 **Fig. 2.** Permeate flux against CF in concentration of watermelon juice by HR98PP (●: 40 bar, ▲: 30 bar; Solid
398 line: estimation, spot: experimental data)

399 **Fig. 3.** Permeate flux against Ln(CF) in concentration of watermelon juice by HR98PP (●: 40 bar, ▲: 30 bar;
400 Solid line: estimation, spot: experimental data).

401 **Fig. 4.** Content and recovery yield of TS in retentate in concentration of watermelon juice by HR98PP (●: 40
402 bar, ▲: 30 bar; filled spot: recovery yield, non-filled spot: content)

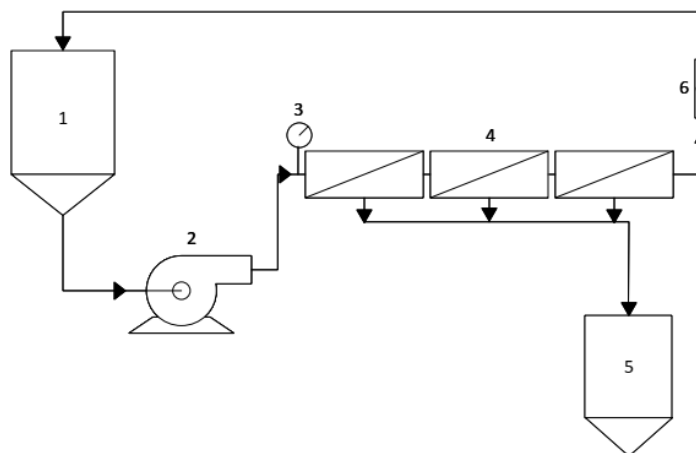
403 **Fig. 5.** Content of TS in permeate in concentration of watermelon juice by HR98PP (●: 40 bar, ▲: 30 bar)

404 **Fig. 6.** Content and recovery yield of lycopene in retentate in concentration of watermelon juice by HR98PP (●:
405 40 bar, ▲: 30 bar; filled spot: recovery yield, non-filled spot: content)

406 **Fig. 7.** Content of lycopene and TS in retentate vs. operating time in concentration of watermelon juice by
407 HR98PP. Plot: experiment (at 40 bar, ○: lycopene, Δ: TS; and at 30 bar, □: lycopene, +: TS). Line: calculation (at 40
408 bar: —: lycopene, ---: TS; at 30 bar, -----: lycopene, -.-.: TS)

409

410



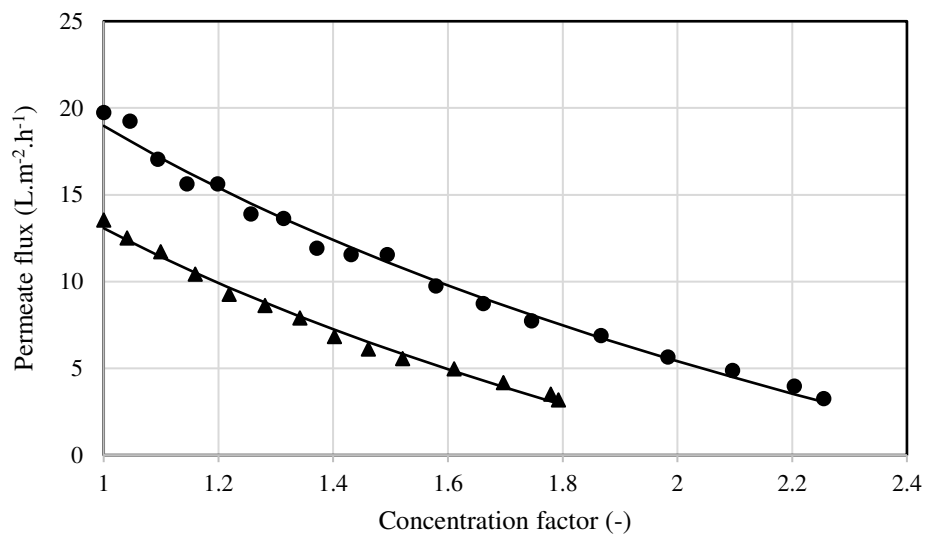
411

412

Fig. 1. Schema of flat and frame pilot LabstakM20 system. 1: feed tank, 2: pump, 3: pressure gauge, 4:

413

membranes, 5: permeate tank, 6: flowmeter



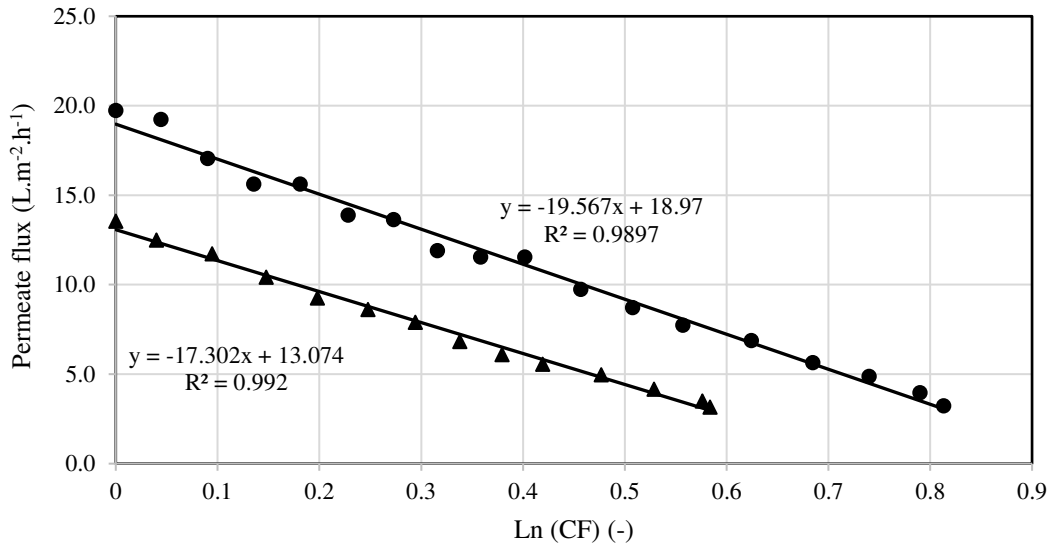
414

415

Fig. 2. Permeate flux against CF in concentration of watermelon juice by HR98PP (●: 40 bar, ▲: 30 bar;

416

Solid line: estimation, spot: experimental data)



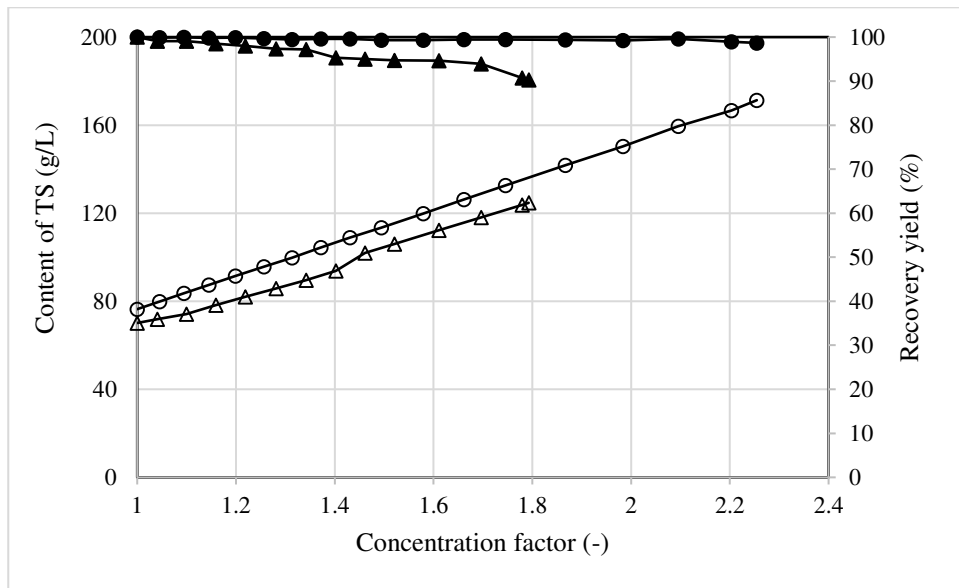
417

418

Fig. 3. Permeate flux against Ln(CF) in concentration of watermelon juice by HR98PP (●: 40 bar, ▲: 30

419

bar; Solid line: estimation, spot: experimental data).



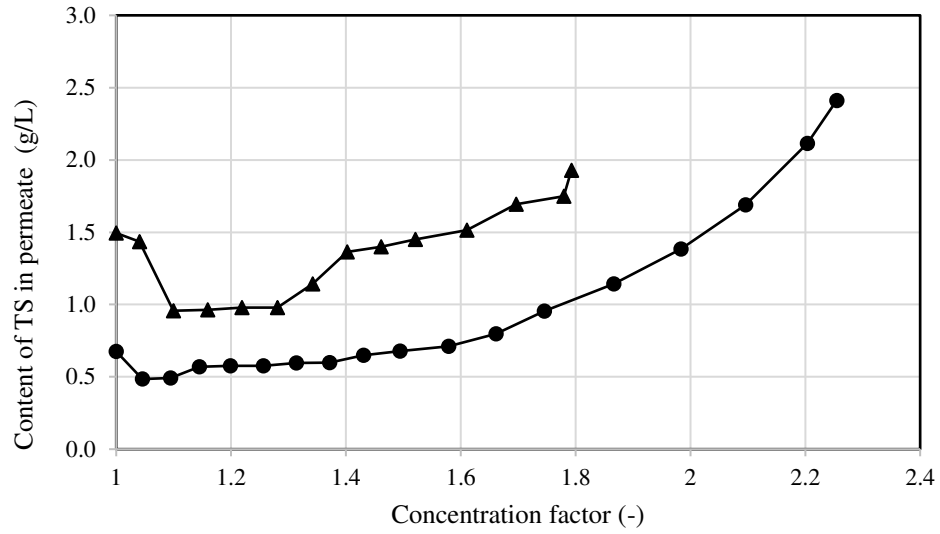
420

421

Fig. 4. Content and recovery yield of TS in retentate in concentration of watermelon juice by HR98PP (●: 40

422

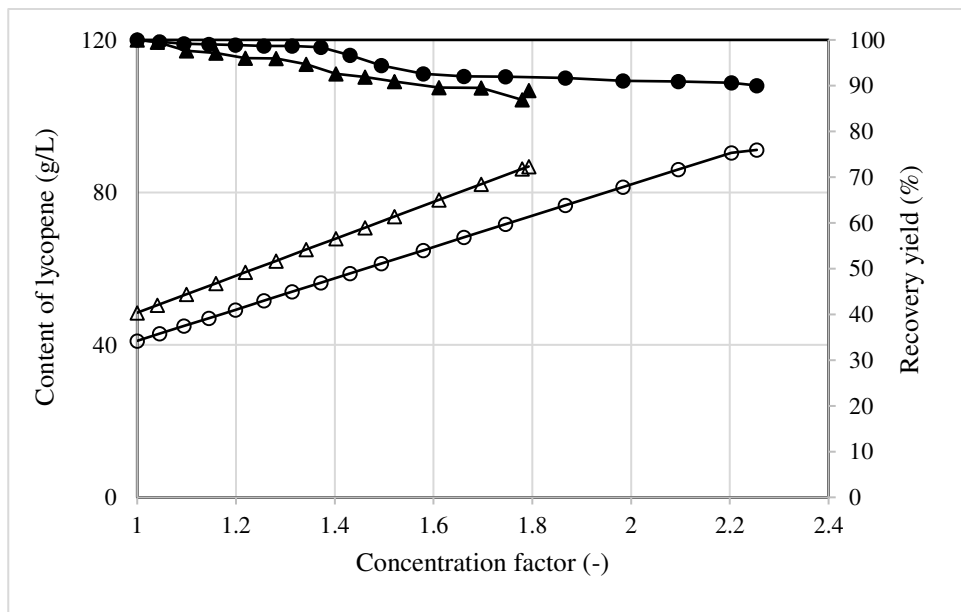
bar, ▲: 30 bar; filled spot: recovery yield, non-filled spot: content)



423

424

Fig. 5. Content of TS in permeate in concentration of watermelon juice by HR98PP (●: 40 bar, ▲: 30 bar)



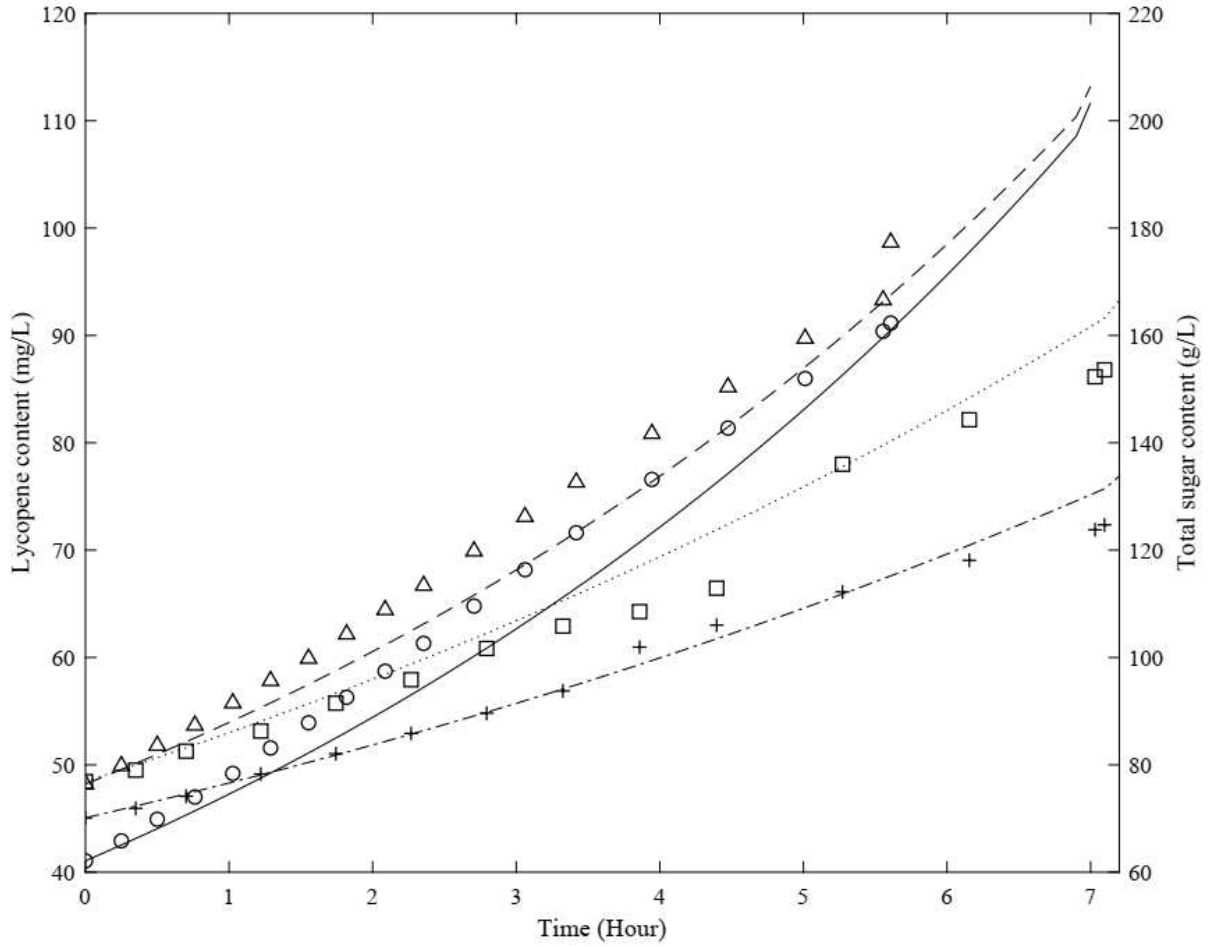
425

426

427

Fig. 6. Content and recovery yield of lycopene in retentate in concentration of watermelon juice by HR98PP

(●: 40 bar, ▲: 30 bar; filled spot: recovery yield, non-filled spot: content)



428

429 **Fig. 7.** Content of lycopene and TS in retentate vs. operating time in concentration of watermelon juice by

430 HR98PP. Plot: experiment (at 40 bar, ○: lycopene, Δ: TS; and at 30 bar, □: lycopene, +: TS). Line: calculation (at

431 40 bar: —: lycopene, ---: TS; at 30 bar,: lycopene, - . - .: TS)

432

TABLE LEGENDS

433 **Table 1.** Flux expressions of Hermia models

434 **Table 2.** Estimation of parameters of model of permeate flux in concentration of water melon juice

435 **Table 3.** Models fitting accuracy for concentration of watermelon juice by HR98PP

436 **Table 4.** Summary of concentration of watermelon juice by HR98PP membrane.

437

438

439

Table 1. Flux expressions of Hermia models

Fouling mechanism	n value	Derivative equation
Complete pore blocking	2	$\ln(J^{-1}) = \ln(J_0^{-1}) + kt$
Standard pore blocking	1.5	$J^{-0,5} = J_0^{-0,5} + kt$
Intermediate pore blocking	1	$J^{-1} = J_0^{-1} + kt$
Cake formation	0	$J^{-2} = J_0^{-2} + kt$

J and J_0 (L/m²h) are the permeate flux at t (h) of operating time and initial time, respectively.

440

441

Table 2. Estimation of parameters of model of permeate flux in concentration of water melon juice

Operating pressure (bar)	k (L.m⁻².h⁻¹)	α	R²	RMSE
30	17.302	2.13	0.992	0.2921
40	19.669	2.63	0.9898	0.5061

442

443

Table 3. Models fitting accuracy for concentration of watermelon juice by HR98PP

Pressure		Cake filtration	Intermediate blocking	Standard blocking	Complete blocking
30 bar	k_n	0.00006	0.0023	0.2024	0.0385
	R ²	0.8568	0.9557	0.986	0.9964
	RMSE	4.6947	1.4839	0.4437	0.1524
40 bar	k_n	0.00003	0.0019	0.2740	0.0169
	R ²	0.7164	0.8806	0.9462	0.9856

RMSE 4.8326 6.995 1.7959 0.5889

444

445

Table 4. Summary of concentration of watermelon juice by HR98PP membrane.

Operating pressure (bar)	Fresh juice			Concentrate juice			Recovery yield			CF	FI	RI
	TS ^a	Ly ^b	AC ^c	TS ^a	Ly ^b	AC ^c	TS ^a	Ly ^b	AC ^c			
30	70.12	48.46	70.81	114.53	76.54	88.86	90.32	86.90	70.11	1.79	67.11	95.72
40	76.41	41.05	67.83	171.31	83.90	125.74	98.67	90.03	82.39	2.25	76.64	96.12

a: g/L, b: mg/L, c: mg TEAC/L

446